Numerical and Experimental Studies of a Novel Converging Stepped Ferrofluid Seal

Xiaolong Yang[1,2], Peng Sun[1], Fan Chen[1], Fuxiang Hao[1], Decai Li[3], and Peter J. Thomas[2]

[1]School of Mechanical Engineering, Guangxi University of Science and Technology, Liuzhou 545006, China
[2]School of Engineering, University of Warwick, Coventry CV4 7AL, U.K.
[3]State Key Laboratory of Tribology, Tsinghua University, Beijing 100084, China

To improve the pressure capability of ordinary ferrofluid seals with a large gap, a novel type of converging stepped ferrofluid seals was proposed. The leakage positions and the magnetic field distributions in the sealing gaps of the new device are studied computationally by means of the finite-element method. The theoretical pressure capabilities of the seal are calculated based on a new expression introduced for the particular new seal geometry and for different sealing gaps. Computational results for effects of the radial and axial sealing gaps on the pressure capabilities of the seal are compared to the experimental results obtained from measurements employing a prototype of the proposed new seal. A good agreement between theoretical and experimental results is obtained. It is found that the pressure capabilities of the new seal depend on the height of the radial sealing gap and on the width of the axial sealing gap.

Index Terms— **Converging seal, experimental investigation, ferrofluid, numerical simulation.**

I. Introduction

FERROFLUID seals are non-contact seals that rely on nanomaterial magnetic fluids as the sealing medium. Ferrofluid seals are widely used in aerospace, mechanical, and naval engineering due to, for instance, their advantages of extremely low leakage, long life, and simple design structure [1]–[3]. However, the capability of ferrofluid seals to resist leakage decreases dramatically with the increase of the sealing gap [4]–[6]. Improving the pressure capability of ferrofluid seals, that is, to increase the critical pressure when the leakage occurs, becomes an issue of major importance in the context of high-speed applications which require large sealing gaps [7]–[9].

Here, we discuss a novel ferrofluid seal, based on a stepwise converging labyrinth layout that improves the pressure capabilities in comparison to ordinary magnetic fluid seals with large sealing gaps. The new design differs from the traditional labyrinth seals, in which it is converging and stepped, and its outer enclosure module incorporates two permanent magnets in series connection and pole pieces in parallel connection. The design layout means that the structure features radial and axial sealing gaps which are formed between the pole pieces and the stepped shaft as will be discussed in detail in the remainder.

There exist numerous studies investigating the performance aspects of ordinary ferrofluid seals with less than 0.3 mm small gap [10]. Examples include the numerical results of the magnetic fluid seal with small sealing gap by Sarma [11] and Radionov *et al.* [12] and the experimental results on the pressure distribution mechanism of the ordinary magnetic fluid seal by Szczęch [13] and Wang and Li [9]. However, the research results were fewer besides the pressure capacities of the diverging stepped magnetic fluid seals with a large sealing gap by Yang and Li [14]. However, corresponding investigations for seals based on a stepped seal layout appear substantially less frequently in [15]–[17]. Here, a formula for the newly designed converging, stepped magnetic fluid seal is presented and applied to the context of experimental tests involving a prototype of the newly designed seal. The leakage positions and the magnetic field distributions in the sealing gaps of our new seal are studied by means of the finite-element method. Predictions obtained for the influence of different radial sealing gap heights and axial sealing gap widths on the pressure capabilities of the seal are compared to the experimental results. The current investigation yields important benchmark data that will be of relevance in the context of the design of similar converging stepped ferrofluid seals with large gaps.

II. Converging Stepped Ferrofluid Seal Formula

Under ordinary conditions, the Bernoulli equation of ferrofluids can be expressed by following formula [2]

$$P + \frac{1}{2}\rho_f V^2 + \rho_f g h - \mu_0 \int_0^H M dH = C \tag{1}$$

where P is the composite pressure of ferrofluids; h, ρ_f, V, and M are the reference height, the density, the velocity, and the magnetization of ferrofluids; g is the gravitational acceleration; μ_0 is the vacuum permeability; H is the external magnetic field strength; and C is the constant. For the static pressure in ferrofluid seals, the effect of velocity on ferrofluid seals can be neglected and the gravity effect in the sealing gap should also be ignored. So, the total sealing capability of a ferrofluid seal is simplified into the following expression:

$$\begin{aligned}\Delta P &= \mu_0 M_S \sum_{i=1}^{N} \left(H^i_{\max} - H^i_{\min}\right) \\ &= M_S \sum_{i=1}^{N} \left(B^i_{\max} - B^i_{\min}\right)\end{aligned} \tag{2}$$

Manuscript received October 1, 2018; revised December 12, 2018; accepted December 27, 2018. Date of publication January 28, 2019; date of current version February 15, 2019. Corresponding author: X. Yang (e-mail: 09116324@bjtu.edu.cn).

Color versions of one or more of the figures in this paper are available online at http://ieeexplore.ieee.org.

Digital Object Identifier 10.1109/TMAG.2019.2892358

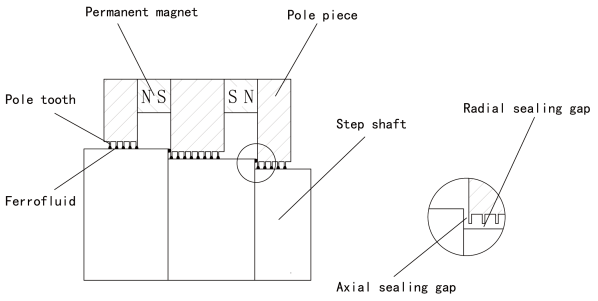

Fig. 1. Schematic of the 2-D physical model of converging stepped ferrofluid seal. The magnified region of the sketch without ferrofluid, to the right, illustrates the nomenclature of axial and radial sealing gaps used throughout this paper.

where $H^i_{\max}$ and $H^i_{\min}$ and $B^i_{\max}$ and $B^i_{\min}$ are, respectively, the maximum and minimum magnetic field strengths and the maximum and minimum magnetic flux densities under the ith pole tooth, while N is the total number of sealed poles.

We express the total sealing capability of the converging stepped magnetic fluid as

$$\Delta P_{\mathrm{c}\max} = \sum_{j=1}^{N} (P_{ja} + \lambda P_{jr}). \tag{3}$$

In (3), P_{ja} and P_{jr} are the pressure capabilities of the ferrofluid seal in the radial and in the axial sealing gaps formed by the jth pole piece and the stepped shaft. We assume that when $P_{ja} < P_{jr}$ then $\lambda = 1$ and, otherwise, $\lambda = 0$. That is, the overall pressure capability of the seal is assumed to be equal to the sum of the axial and radial pressure capabilities when the axial capability is below the radial capability. However, the overall pressure capability is solely governed by the axial capability when this is larger than the radial capability. The values for P_{ja} and P_{jr} can be calculated from (2). The discussion following below will reveal that (3) yields a good agreement with the experimental data to be presented.

III. Structure Design of the Converging Stepped Ferrofluid Seal

The design layout of our new seal is illustrated in Fig. 1. The seal has radial and axial gaps as indicated in Fig. 1. The radial gaps are located between the pole teeth and the shaft in Fig. 1, and the clearance is referred to as the gap height. The axial gaps are located between the pole pieces and the vertically aligned sections of the shaft shown in Fig. 1, and the clearance is referred to as the gap width. In order to study the leakage position of the converging stepped ferrofluid sealing structure and to verify its pressure capability, a 2-D prototype was built. The prototype had the basic structural parameters summarized in Table I. Two NdFeB permanent magnets were integrated in the seal, as shown in Fig. 1. The coercive force and permeability of the magnets are $H_c = 1.356 \times 10^6$A/m and 1.05, respectively. The pole pieces and the stepped shaft are made from 2Cr13. The sealing medium is an oil-based ferrofluid with a saturation magnetization of 30.7 kA/m.

TABLE I
Parameters of the New Converging Stepped Ferrofluid Seal

Item	Value
Inner radius of the1/2/3 pole piece (mm)	19.6/18.1/16.6
Outer radius of the 1/2/3 pole piece (mm)	30
Length of the 1/2/3 pole piece (mm)	5/8/5
Permanent magnets length	5
radius of each permanent magnets	48
Outer radius of each permanent magnets	60
Number of teeth under the 1/2/3pole piece	5/8/5
Axial width of pole teeth (mm)	0.2
Axial sealing gap width (mm)	0.4/0.5/0.6/0.7
Radial sealing gap height (mm)	0.4/0.6/0.8/1.0
Slot depth (mm)	0.7
Slot width (mm)	0.8

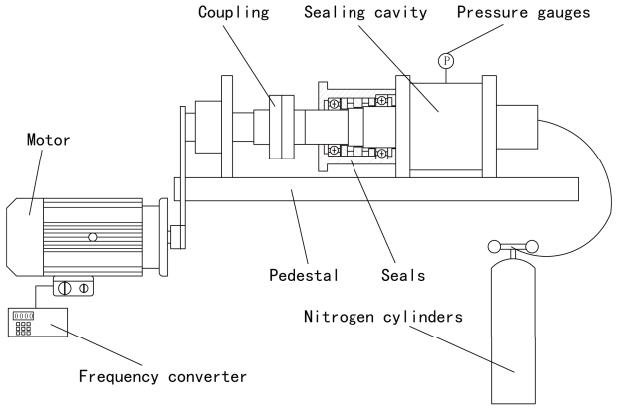

Fig. 2. Converging stepped ferrofluid seal test bed.

A finite-element simulation of the design shown in Fig. 1 was performed by means of the ANSYS software Emag package using the data given in Table I and the material properties of the magnets, of the pole pieces and the shaft mentioned above. The computations were performed using an intelligent mesh with precision 1. The applied boundary condition is that the magnetic field lines are parallel to the boundaries of the computational domain enclosing the 2-D physical model. The magnetic field distributions in the sealing gap were then obtained by the ANSYS solver.

IV. Experimental Process and Method

For the verification of the theoretical results for the pressure capability of our new seal, a test rig as illustrated in Fig. 2 was developed with the structural parameters, as given in Table I. The setup shown in Fig. 2 consists of nitrogen cylinders, pressure gauges, sealing cavity, seals, motors, and valves.

The experimental procedure proceeded as follows. Initially, the new sealing device was mounted securely within the sealing cavity. The stepped shaft of the new seal is connected with the rotating shaft of the motor on the test bed through a mechanical coupling. The volume of the ferrofluid injected into the sealing gap is 5 mL which is sufficient for seal. Then, the sealed chamber is pressurized at 0.1 atm with helium to enable a helium mass spectrometer leak detector to monitor the leakage of the sealing device. Thereafter, the motor was started and allowed running for 30 min at a speed of 1000 r/min. Then, nitrogen gas is slowly inserted into the sealing chamber in small successive steps of 0.1 atm separated by time intervals of 2 min, up to a maximum critical pressure. The pressure level when the helium mass spectrometer leak detector registers leakage is recorded to obtain the maximum pressure capability of the seal. Following the experiment, the sealing structure was dismantled. The shaft assembly was removed, carefully cleaned, and machined to obtain a seal with new gap dimensions. The modified structure was then reassembled for the next experimental run to investigate the effects of the radial sealing gap height and axial sealing gap width on the capabilities of the stepped converging stepped ferrofluid seal.

V. Results and Discussion

A. Determination of Leakage Position

In order to accurately evaluate the theoretical pressure capabilities of our new seal, it is necessary to determine that the location of the seal where leakage is most likely to occur first. To this end, the following assumptions have been made. It is assumed that once the seal fails, the leakage channel is straight in both the radial and axial sealing gaps. Moreover, it is assumed that the leakage location coincides with the location of the minimum magnetic field gradient. The sealing gaps are divided into equidistant leakage channels of 0.1 mm width. For instance, if both the radial and the axial gaps are 0.4 mm, the leakage channels are located at distances of 0, 0.1, 0.2, 0.3, and 0.4 mm from the stepped shaft, in the radial and axial sealing gaps; the magnetic field distribution for this case is shown in Figs. 3 and 4.

Fig. 3 shows that as the tracking position proceeds from the shaft to the pole tooth side, the magnetic flux densities in the left, middle, and right radial sealing gaps increase. This behavior corresponds to the results obtained for the axial sealing gap. However, when the tracking position proceeds from the shaft to the pole tooth side, then, the magnetic flux density differences increase and, in this case, this behavior is different in comparison to that of the axial sealing gaps. This implies that the magnetic flux densities and the magnetic flux density differences are larger when the most probable leakage location is far from the stepped shaft. It indicates that the leakage occurs at a location near the shaft side in the radial sealing gap. The reason is that the pole teeth are located closer to the permanent magnet than the shaft surface. The magnetic field intensity and the magnetic flux density difference near the rotating shaft side are smaller than the values near the pole teeth. Thus, the pressure capability of the ferrofluid seal on the stepped axis side is weaker, and it is also the most probable leakage location.

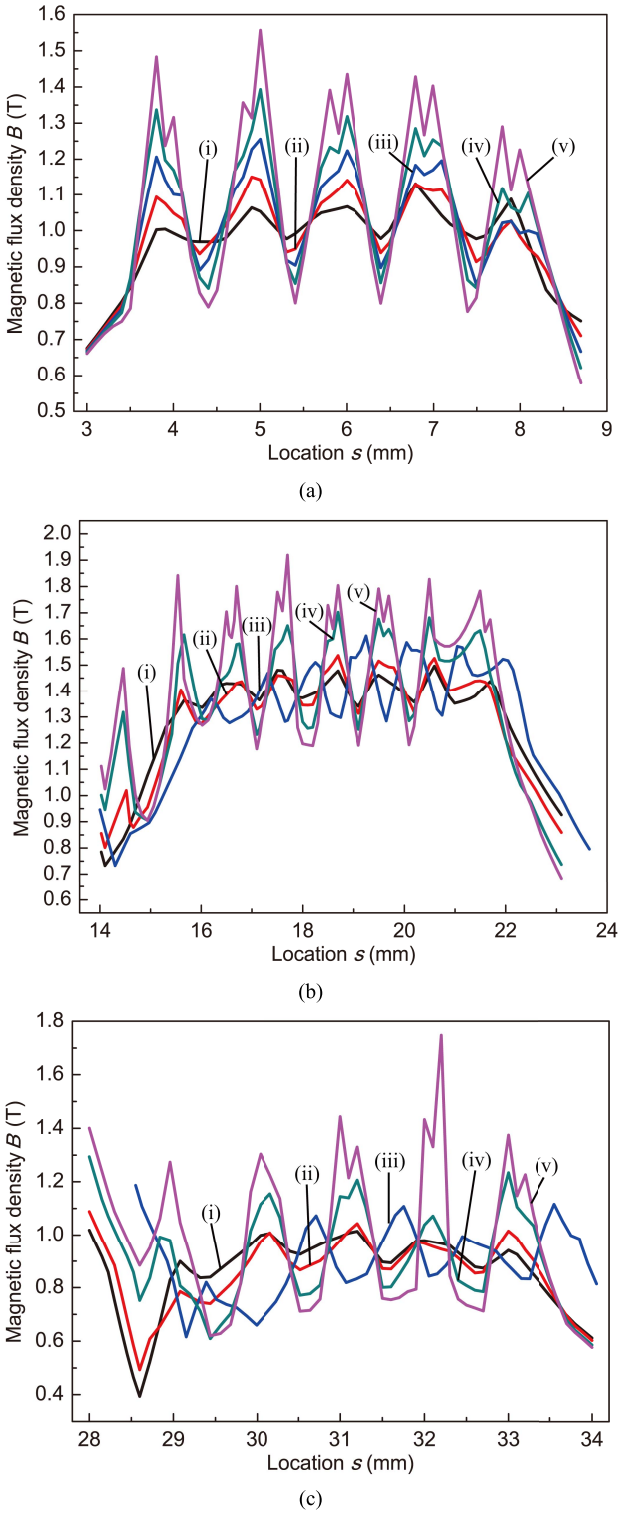

Fig. 3. Magnetic field distributions in (a) left, (b) middle, and (c) right radial sealing gaps of the converging stepped ferrofluid seal. Magnetic field distribution (i) at the stepped shaft side, (ii) at a distance of 0.1 mm from the stepped shaft, (iii) at the middle position of the axial sealing gap, (iv) at the 0.3 mm position far from the stepped shaft, and (v) on the pole piece side.

Fig. 4 reveals that the magnetic flux densities in the middle and right axial gaps increase as the tracking location moves away from the shaft toward the pole tooth side. The reason for this increase is that the magnetic flux density is stronger near the permanent magnet. However, the differences in the

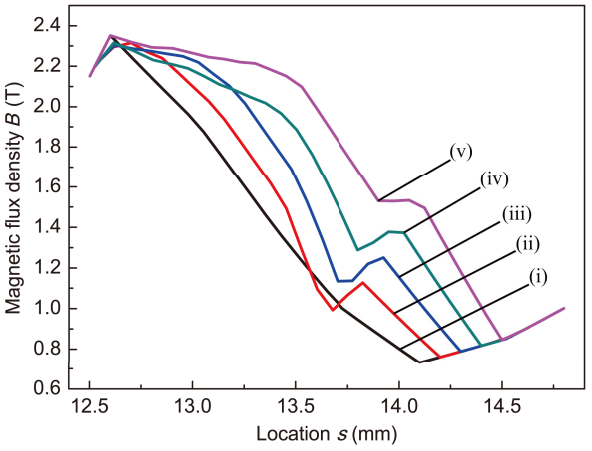

(a)

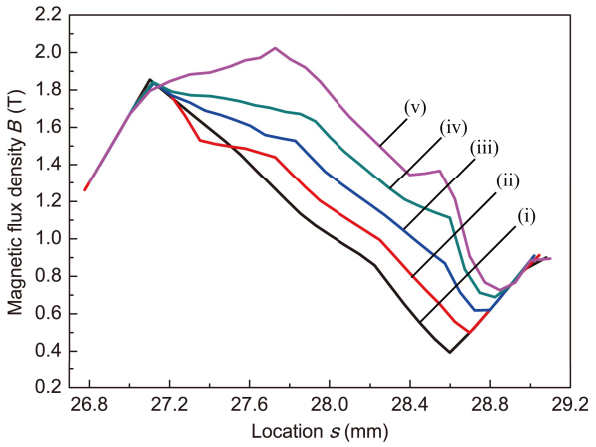

(b)

Fig. 4. Magnetic field distributions in (a) middle and (b) right axial sealing gaps of the converging stepped ferrofluid seal. Magnetic field distribution locating (i) near the stepped shaft side, (ii) at a distance of 0.1 mm from the stepped shaft, (iii) at the middle position of the axial sealing gap, (iv) at a distance of 0.3 mm from the stepped shaft, and (v) on the pole piece side.

value of the magnetic flux densities in the middle and right axial gaps first reduce and then increase. Its minimum value is located at the center of the axial sealing gap. This implies that leakage most likely occurs at the center of the axial sealing gap. The main reason for this is that the maximum magnetic flux density at the middle location of the axial sealing gap is minimum relative to the maximum value of other leakage locations and the magnetic field is stronger near the pole and the side of the rotating shaft. Thus, the magnetic flux density difference is smallest at the middle position of the axial sealing gap, and it is also the most likely location where leakage is to occur first.

B. Effect of the Radial Sealing Gap

The theoretical pressure capability of the new seal is related to the magnetic field intensity difference or magnetic flux density difference in its radial and axial sealing gaps. In order to obtain the effect of the radial sealing gap on the theoretical pressure capability of the seal, it is necessary to calculate the magnetic field intensity or magnetic flux density distribution in the radial and axial sealing gaps of the seal structure.

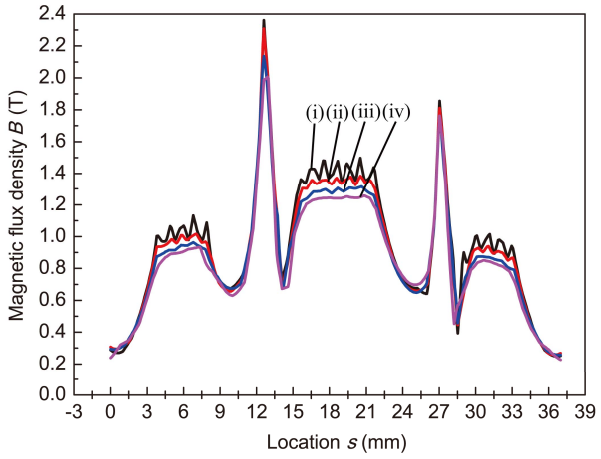

Fig. 5. Magnetic field distributions for different radial sealing gaps. (i) 0.4 mm. (ii) 0.5 mm. (iii) 0.6 mm. (iv) 0.7 mm.

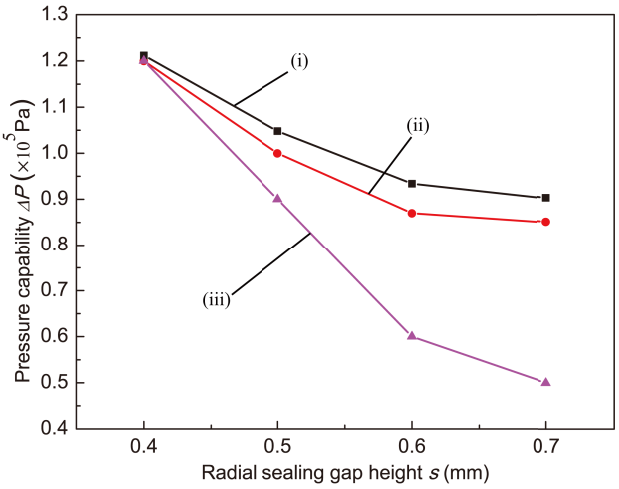

Fig. 6. Critical leakage pressure ΔP as a function of height s of the radial sealing gaps. (i) Theoretical values for the new converging stepped ferrofluid seal. (ii) Experimental values for the new converging stepped ferrofluid seal. (iii) Experimental values for the ordinary ferrofluid seal.

Fig. 5 displays the magnetic field distribution for an axial sealing gap of 0.4 mm and for radial sealing gaps between 0.4 and 0.7 mm.

It is straightforward to verify that the maximum magnetic flux density in the axial sealing gap is larger than that in the radial sealing gap. The reason is that for constant width of the axial sealing gap and larger height of the radial sealing gap, the magnetic reluctance in the radial sealing gap is lower than that in the axial sealing gap. According to the law of magnetic force, the maximum magnetic flux density in the axial gap of the magnetic circuit is, therefore, larger than that in the radial gap.

Based on the magnetic field distributions and the theoretical description of the converging stepped magnetic fluid seal, its pressure capabilities can be calculated. Fig. 6 displays a comparison between theoretical and experimental data of the critical leakage pressure ΔP for an axial sealing gap of 0.4 mm width and for different radial sealing gaps s in the range from 0.4 to 0.7 mm.

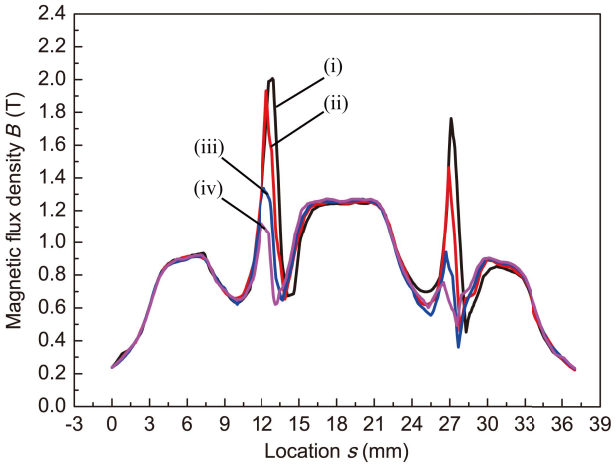

Fig. 7. Magnetic field distributions for different axial sealing gaps. (i) 0.4 mm. (ii) 0.6 mm. (iii) 0.8 mm. (iv) 1.0 mm.

Fig. 6 shows that the theoretical and experimental pressure capabilities of the seal decrease with increasing width of the radial sealing gap. This behavior is analogous to that obtained for the change of the pressure capacity of ordinary magnetic fluid seals. It reveals that the sealing action in both the axial and radial sealing gaps contributes to the overall sealing capability. The reason is that for constant axial sealing gap width, with concurrently larger radial sealing gap height and for, otherwise, identical structural sealing parameters, the magnetic reluctance of the sealing gap increases with an increase of the radial sealing gap height. An increasing magnetic reluctance in the magnetic circuit will cause a decrease of the magnetic flux density in the radial and axial sealing gaps according to the law of magnetic circuit. Finally, the decreasing magnetic flux density will result in a reduced total pressure capacity of the converging stepped ferrofluid seal.

Fig. 6 shows that the maximum discrepancy between the theoretical and experimental values of the critical leakage pressure of the seal is less than 0.1 atm which represents a good agreement. This also corroborates our above-mentioned assumptions from Section V-A regarding the leakage locations in the radial and axial sealing gaps and corroborates the validity of (3).

Fig. 6 also shows that the critical leakage pressure of the converging stepped ferrofluid seal is equal to that of the ordinary ferrofluid seal when the radial sealing gap is 0.4 mm. The reason is that when the radial sealing gap height is equal to the axial sealing gap width, the ferrofluid seals in the axial sealing gap do not contribute to the overall sealing capability. When the radial sealing gap is larger than 0.4 mm, the critical leakage pressure of the converging stepped ferrofluid seal is larger than that of the ordinary ferrofluid seal. This indicates that the ferrofluid seals in the axial sealing gaps contribute to the total pressure capability of the converging stepped ferrofluid seal.

C. Effect of the Axial Sealing Gap

Fig. 7 displays the magnetic field distribution for a radial sealing gap of 0.7 mm width and different values for the width of the axial sealing gaps.

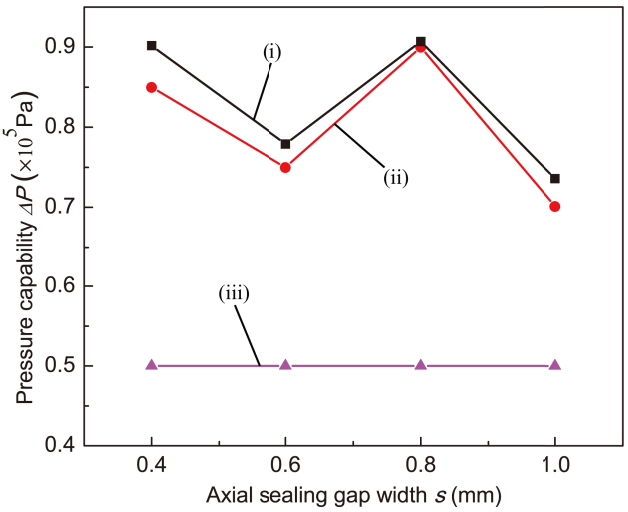

Fig. 8. Critical leakage pressure ΔP as a function of width S of the axial sealing gaps. (i) Theoretical values for the new converging stepped ferrofluid seal. (ii) Experimental values for the new converging stepped ferrofluid seal. (iii) Experimental values for the ordinary ferrofluid seal.

Fig. 7 reveals that when the axial sealing gap width increases from 0.4 to 1.0 mm, the magnetic flux density in the axial sealing gap of the seal decreases with an increase of the width of the axial sealing gap. The reason is that the magnetic reluctance of the sealing gap increases with increasing width of the axial sealing gap and the magnetic flux density in the axial sealing gap decreases according to the magnetic circuit law.

Based on the magnetic field distributions and the theoretical description of the seal, its pressure capacity can be calculated for a constant radial sealing gap of width 0.7 mm. Fig. 8 shows a comparison of experimental and theoretical results obtained for four different values of the width of the axial sealing gap ranging between 0.4 and 1.0 mm.

Fig. 8 shows that the maximum error between the theoretical and experimental values does not exceed 0.05 atm reflecting a good agreement. This also shows that the assumptions of the leak location in the radial and axial sealing gaps are reasonable and it corroborates the validity of (3).

Fig. 8 reveals that for the constant height of the radial seal gap, the pressure resistance of the seal initially decreases with increasing axial gap width, followed by an increase upon which it begins to decrease once again. This behavior differs from the sealing resistance of ordinary magnetic fluid seals. Fig. 8 shows that the pressure capability decreases by about 0.1 atm upon increasing the width of the axial seal gap from 0.4 to 0.6 mm. When the width of the axial seal gap is increased from 0.6 to 0.8 m, the pressure capability increases with increasing axial seal gap width by approximately 0.15 atm. Above 0.8 mm, the pressure resistance of the seal begins to decrease with a further increase of the width of the axial gap of the seal. The reason for this phenomenon is that the gradient difference of the magnetic field in the axial gap of the seal is larger than that within the radial seal gap when the width of the axial gap is less than or equal to the height of the radial seal gap. According to the pressure resistance theory of the seal, its pressure capability depends on the pressure capability

in the axial gap, and the magnetic fluid seal in the radial sealing gap is ineffective. Therefore, the pressure resistance of the converging stepped magnetic fluid seal decreases with the increase of the width of the axial sealing gap from 0.4 to 0.6 mm. When the width of the axial sealing gap is increased from 0.6 to 0.8 mm, the gradient difference of the magnetic field in the axial seal gap is less than that within the radial seal gap. This means that the magnetic fluid seals in both the radial and axial sealing gaps contribute to the overall sealing capability in agreement with our assumptions and (3). Upon increasing the axial gap width from 0.6 to 0.8 mm, the pressure capability of the seal will, therefore, increase instead of decrease. When the width of the axial gap increases further, from 0.8 mm and therewith being larger than the height of the radial sealing gap, the pressure capability of the seal decreases with an increasing axial gap width according to the law of magnetic circuits.

Fig. 8 also shows that the critical leakage pressure of the converging stepped ferrofluid is dramatically larger than that of the ordinary ferrofluid seal. This indicates that the ferrofluid seals in the axial sealing gaps contribute to the total pressure capacity of the converging stepped ferrofluid seal. Hence, selecting the proper axial gap width is significance to improve the ordinary ferrofluid seals.

VI. Conclusion

A novel converging stepped magnetic fluid seal has been designed, and the magnetic field distribution within the seal has been analyzed by means of the finite-element method. Assumptions made for the leakage position in the sealing gap of the converging stepped ferrofluid seal have been verified. The theoretical value of the pressure capability, i.e., the critical leakage pressure, of the new seal was calculated and compared to the experimental values obtained from measurements employing a prototype of the seal. The results show that the leakage positions in the radial sealing gaps are located in the vicinity of the shaft while those in the axial sealing gaps are located at the centers of the gaps. The experimental and theoretical values for the critical leakage pressures of the new seal are found to be in a good agreement. This shows that the assumptions for the leakage location in the radial and axial sealing gaps and the theory of the converging stepped magnetic fluid seal are correct. In particular, the pressure capability of the new seal is not only affected by the radial sealing gap but it also depends on axial sealing gaps. The maximum critical capability of the new type converging stepped ferrofluid seal is approximately two times of the ordinary ferrofluid seal, and it is an effective method to improve the critical pressure of ferrofluid seals.

Acknowledgment

This work was supported in part by the National Nature Science Foundation of China under Grant 51375039, in part by the Science and Technology Project of Guangxi Province under Grant 2016GXNSFBA380213, in part by the Innovation Project of Guangxi Graduate Education under Grant YCSW2018200, and in part by the Science and Technology Project of Liuzhou under Grant 2017BC20204.

References

[1] W. Yang, P. Wang, R. Hao, and B. Ma, "Experimental verification of radial magnetic levitation force on the cylindrical magnets in ferrofluid dampers," *J. Magn. Magn. Mater.*, vol. 426, pp. 334–339, Mar. 2017.

[2] R. E. Rosensweig, *Ferrohydrodynamics*. New York, NY, USA: Dover Publications, 2002.

[3] Z. Meng, Z. Jibin, and H. Jianhui, "An analysis on the magnetic fluid seal capacity," *J. Magn. Magn. Mater.*, vol. 303, no. 2, pp. e428–e431, Aug. 2006.

[4] M. Kroell, M. Pridoehl, G. Zimmermann, L. Pop, S. Odenbach, and A. Hartwig, "Magnetic and rheological characterization of novel ferrofluids," *J. Magn. Magn. Mater.*, vol. 289, pp. 21–24, Mar. 2005.

[5] M. Szczęch and W. Horak, "Numerical simulation and experimental validation of the critical pressure value in ferromagnetic fluid seals," *IEEE Trans. Magn.*, vol. 53, no. 7, Jul. 2017, Art. no. 4600605.

[6] F. Chen, X. Yang, S. Gao, and Y. Chen, "Numerical study on key parameters of ferrofluid seal with large gap and two magnetic sources," *Int. J. Appl. Electromagn. Mech.*, vol. 55, no. 3, pp. 535–543, Nov. 2017.

[7] Z. Li and K. Raj, "Effect of vacuum level on evaporation rate of magnetic fluids," *J. Magn. Magn. Mater.*, vol. 289, pp. 43–46, Mar. 2005.

[8] R. Ravaud *et al.*, "Radial stiffness of a ferrofluid seal," *IEEE Trans. Magn.*, vol. 45, no. 10, pp. 4388–4390, Oct. 2009.

[9] Z. Wang and D. Li, "Theoretical analysis and experimental study on loading process among stages of magnetic fluid seal," *Int. J. Appl. Electromagn. Mech.*, vol. 48, no. 1, pp. 101–110, 2015.

[10] D. Li, H. Xu, X. He, and H. Lan, "Study on the magnetic fluid sealing for dry roots pump," *J. Magn. Magn. Mater.*, vol. 289, pp. 419–422, Mar. 2005.

[11] M. S. Sarma, P. Stahl, and A. Ward, "Magnetic-field analysis of ferrofluidic seals for optimum design," *J. Appl. Phys.*, vol. 55, no. 6, pp. 2595–2597, Apr. 1984.

[12] A. Radionov, A. Podoltsev, and A. Zahorulko, "Finite-element analysis of magnetic field and the flow of magnetic fluid in the core of magnetic-fluid seal for rotational shaft," *Procedia Eng.*, vol. 39, no. 11, pp. 327–338, Dec. 2012.

[13] M. Szczęch, "Experimental study on the pressure distribution mechanism among stages of the magnetic fluid seal," *IEEE Trans. Magn.*, vol. 54, no. 6, Jun. 2018, Art no. 4600507.

[14] X. L. Yang and D. C. Li, "Experimental investigation of diverging stepped magnetic fluid seals with large sealing gap," *Int. J. Appl. Electromagn. Mech.*, vol. 50, no. 3, pp. 407–415, Mar. 2016.

[15] Z. Szydlo, W. Ochoński, and B. Zachara, "Experiments on magnetic fluid rotary seals operating under vacuum conditions," *Tribotest*, vol. 11, no. 4, pp. 345–354, Jun. 2005.

[16] J. Yao, J. Chang, D. Li, and X. Yang, "The dynamics analysis of a ferrofluid shock absorber," *J. Magn. Magn. Mater.*, vol. 402, pp. 28–33, Mar. 2016.

[17] M. D. Volder and D. Reynaerts, "Development of a hybrid ferrofluid seal technology for miniature pneumatic and hydraulic actuators," *Sens. Actuators A, Phys.*, vol. 152, no. 2, pp. 234–240, Jun. 2009.